

Chemical state of Ag in Conducting Bridge Random Access Memory cells: a depth resolved X-ray Absorption Spectroscopy investigation.

F d'Acapito*, E Souchier[@], P Noe[@], P Blaise[@], M Bernard[@], V Jousseau[@]

* CNR-IOM-OGG c/o ESRF, LISA CRG, 71 Avenue des Martyrs, Grenoble (France),
dacapito@esrf.fr

[@] Univ. Grenoble Alpes, CEA, LETI, MINATEC Campus, 17 Rue des Martyrs, Grenoble (France)

E-mail: dacapito@esrf.fr

Abstract. Conducting Bridge Random Access Memories (CBRAM) are a promising substitute for FLASH technology but problems with limited retention of the low resistance *ON* state still hamper their massive deployment. Depth resolved X-ray Absorption Spectroscopy has been used to describe the chemical state of the atoms of the active electrode (in this case Ag) and to reveal the role of Sb as stabilizer of the metallic state.

1. Introduction

Conducting Bridge Random Access Memories (CBRAM) represent one of the possible substitutes for the FLASH technology below the 22 nm node [1]. These memory cells are based on a chalcogenide layer (namely GeS₂) sandwiched between two metallic electrodes: one inert (usually W or Pt) and the other active (Ag, Cu). Upon application of an electric field the ions from the active electrode migrate in the chalcogenide layer and eventually form metallic filaments that reduce considerably the resistance of the cell to the Low Resistance State (*ON* state). The application of an opposite electric field leads to the partial dissolution of the wire and to a regain of cell resistivity to the High Resistance State (*OFF* state). CBRAMs offer good scalability but suffer from the instability of the *ON* state due to the spontaneous dissolution of the metallic bridge in the surrounding matrix with time [2] and this represents a severe limitation in the use of these memories in a multilevel configuration. Recently [3] it has been reported that the addition of Sb to the chalcogenide layer has beneficial effects on the retention of the *ON* state. For this study REFlection Extended X-ray Absorption Fine Structure (ReFlEXAFS) technique [4, 5, 6, 7, 8] has been used to derive information on the chemical state of Ag below the active electrode and in the chalcogenide layer. These findings shed light on the formation process of the wires and on the role of Sb in stabilizing the metallic phase for Ag.

2. Experimental

Two samples, consisting in Ag-doped and Ag+Sb-doped GeS₂ chalcogenide thin films, were prepared by co-sputtering from GeS₂ and Sb pure targets over a W bottom electrode of 25



nm deposited on Si. The chalcogenide layer had a thickness of 50 nm and Sb was introduced at a 10 % level. Ontop of the layer a 3 nm-thick top Ag electrode was deposited in order to create a real memory cell. One of the cells underwent a serie of 20 resistive switching cycles before the removal of the Ag top electrode by ion beam etching prior to XAS analysis. The lateral dimensions of all samples were 3×80 mm. In the following the samples will be named SW (switched) and NSW (non-switched).

Samples were measured at the Ag K edge ($E=25514$ eV) in the dedicated experimental station [9] operative at the GILDA beamline at the ESRF [10]. The scattering vector was vertical and the vertical size of the beam was about $50 \mu\text{m}$. The incoming and the reflected beams were measured with ion chambers loaded with Kr gas at 1 atm. The experimental procedure was the same used for investigations on Sb-free samples [11] and for studying the Sb behavior in these samples [10]. For each specimen a reflectivity curve at fixed energy (25600 eV) was first collected (fig.1) and two zones were identified. The *surface* (Σ) regime at an incidence angle of about 0.07° (where the beam was in total external reflection and the extinction length of the beam was estimated to be 4 nm) and the *layer* (Λ) regime at about 0.15° (where the probe beam shines the whole chalcogenide layer). Collecting XAS data at these two values for the incidence angle permitted to realize a depth-sensitive investigation in the zones near the active (Ag) electrode and inside the layer. The data were analyzed with the CARD code [12] in its version 04 that permits the treatment of layered samples [13].

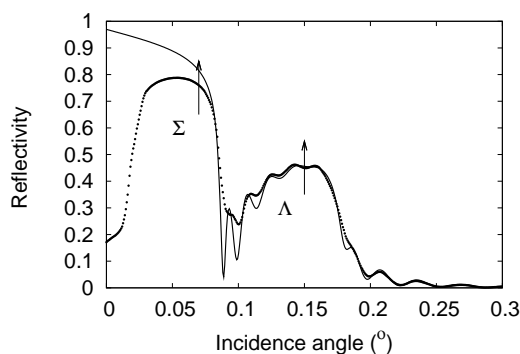


Figure 1. Reflectivity of sample NSW collected at 25600 eV (dots) with the best fitting curve (line). The angles for the Surface (Σ , 0.07°) and Layer (Λ , 0.15°) datasets are marked by arrows.

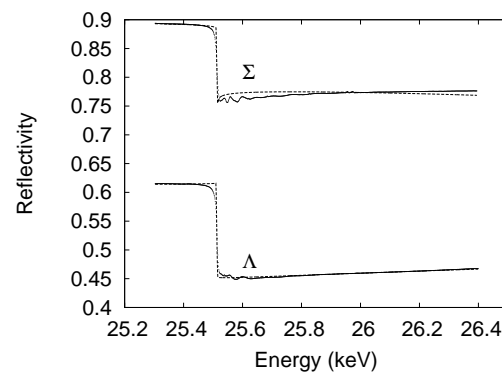


Figure 2. Reflectivity curves of sample NSW collected at Σ and Λ values for the incidence angle (dots) with the best fitting curves (lines).

3. Results

For both SW and NSW samples the reflectivity at fixed angle was fitted to a model consisting in two layers Ag:GeS_x and W above a Si substrate. The W thickness was found to be $t_W = 300 \pm 30$ nm with a roughness $\sigma_W = 0.7 \pm 0.1$ nm and the chalcogenide had $t_{chcalco} = 500 \pm 50$ nm and $\sigma_{chcalco} = 1.9 \pm 0.2$ nm, in good agreement with growth data. From the measured density of the chalcogenide layer ($4.1 \pm 0.3 \text{ g/cm}^3$) a composition $(\text{GeS}_2)_{0.75}(\text{Ag}_2\text{S})_{0.25}$ could be derived. Successively RefEXAFS spectra were collected at each of the two incidence angle values and the reflectivity fits are shown in fig.2. Once having determined the parameters determining the sample reflectivity a set of suitable modified theoretical EXAFS paths were calculated with CARD and used for the quantitative data fitting using the FEFFIT code [14]. As an example, the EXAFS spectra of the NSW sample are shown in fig. 3 whereas the related Fourier Transforms

Sample	Metal Fraction x	R_{AgS} (\AA)	R_{AgAg} (\AA)
NSW- Σ	0.51(5)	2.47(3)	2.86(3)
NSW- Λ	0.37(7)	2.46(3)	2.84(4)
SW- Σ	0.70(5)	2.50(5)	2.86(3)
SW- Λ	0.40(8)	2.46(3)	2.80(5)

Table 1. Main structural parameters derived from the quantitative analysis of the RefEXAFS data; errors on the last digit are in parentheses. A global amplitude reduction factor of 0.95(5) was used as determined from the spectrum of metallic Ag taken in transmission mode. For comparison, the distance measured on the metal foil was $R_{AgAg}=2.880(5)\text{\AA}$. The Debye-Waller factors were $\sigma_{AgS}^2 = 0.0012(5)$ and $\sigma_{AgAg}^2 = 0.0025(5)$

are in fig. 4. The spectra contain two components, a low frequency one due to Ag-S bonds and

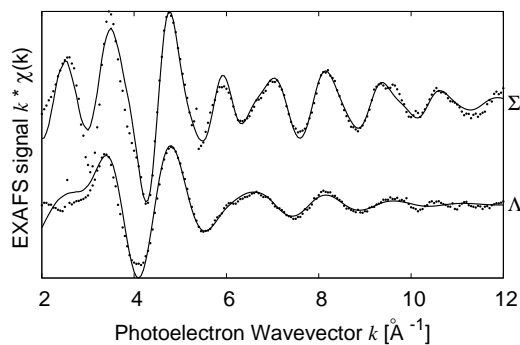


Figure 3. RefEXAFS spectra of the *NSW* sample in Λ and Σ condition obtained from the difference between the reflectivity R and the spline approximant to the atomic background. With this definition these spectra appear to be reversed with respect to standard XAS spectra due to the opposite edge jump.

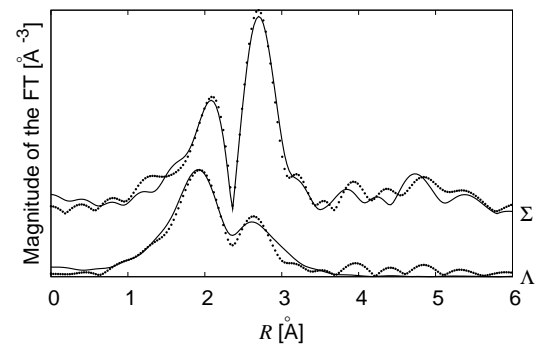


Figure 4. FTs of the previous spectra taken in the interval $2\text{--}12\text{ \AA}^{-1}$. An interpretation of these spectra is not straightforward as the two peaks in the Λ spectrum come from the two AgAg and AgS shells whereas in the case of the Σ spectrum the splitting is dominated by the Ramsauer-Townsend effect [15] on the Ag backscatterer.

a higher frequency one due to Ag-Ag bonds. The data analysis was carried out following the procedure already used for these systems [11, 16] i.e. by mixing a 3-coordinated Ag-sulphide phase plus a 12 coordinated Ag-metal phase with relative weights x and $(1-x)$. Table. 1 resumes the main parameters.

4. Discussion

The RefEXAFS spectra reveal the presence of two kind of bonds for Ag, AgS derived from the Ag ions dispersed in the GeS_2 matrix and AgAg coming from the metallic fraction forming the wires that cause the resistance drop in the *ON* state of the cell. Different values for the metallic fraction are observed in surface and in the layer in the *SW* and *NSW* samples. This shows that the metal fraction already before the switching process is higher near to the active electrode and the same situation is retained after the formation of the conducting wires. As a consequence, the

wires can be described as cones with the base towards the active electrode. This reveals a low diffusivity of Ag and a reduction process faster than the ion migration as already observed in Ref. [17] in $Cu/Al_2O_3/TiN$ cells. In both cases the SW sample has a higher metal amount than the NSW sample revealing that new metal is formed during the switching process that is not completely dissolved during the switching cycles. It is worth noticing that in all cases the metal fraction is sensibly higher if compared with similar samples grown without Sb [11]. This is due to the action of Sb making stable bonds with the available S ions [16] making more difficult the sulphurization of Ag. This leads to an increased retention of the *ON* state by the cell as pointed out by [3]. The AgAg bond length appears to be slightly shorter in the Λ samples respect to Σ and bulk Ag ($R_{AgAg}=2.880(5)\text{\AA}$) probably due to the possible presence of Ag oligomers.

5. Conclusion

Depth resolved XAS has been used to describe the chemical state of Ag ions Conductive Bridge Random Access Memories in their pristine state or after having undergone several switching cycles. The samples analyzed contained Sb in the chalcogenide layer as recent literature [3] reported a beneficial effect of this element on the retention of the *ON* state. The switched sample presents an overall higher metal content than the non switched one, meaning that this process really leads to the formation of new metal after the cell deposition. The metal content is higher below the active electrode, revealing that the cone-shaped filaments have their thicker part towards this part of the sample. The values of metal fraction observed here are sensibly higher than those found on Sb-free samples [11] : having established that Sb forms stable bonds with S in these samples [16], this finding confirms the Sb role in hampering the sulphurization of Ag.

References

- [1] 2013 *International Technology Roadmap for Semiconductors 2013 edition Process Integration, Devices, and Structures*.
- [2] Guy J *et al.* 2014 *Thin Solid Films* **563**
- [3] Vianello E *et al.* 2012 *Proceedings of the IEEE International Electron Devices Meeting (IEDM), San Francisco*
- [4] Barchewitz R and Onori M C V 1978 *J. Phys. C* **11** 4439
- [5] Martens G and Rabe P 1980 *Phys. Stat. Sol. A* **58** 415
- [6] Heald S 1992 *Rev. Sci. Instrum.* **63** 873
- [7] Asakura K, Chun W and Iwasawa Y 2000 *Topics Catal.* **10** 209
- [8] Lützenkirchen-Hecht D and Frahm R 2001 *J. Synchrotron Rad.* **8** 478
- [9] d'Acapito F, Davoli I, Ghigna P and Mobilio S 2003 *J. Synchrotron Rad.* **10** 260
- [10] d'Acapito F, Trapananti A, Torrenzo S and Mobilio S 2014 *Notiziario Neutroni e Luce di Sincrotrone* **19** 14
- [11] Souchier E, d'Acapito F, Noe P, Blaise P, Bernard M and Jousseume V 2015 *Phys. Chem. Chem. Phys.* **17** 23931
- [12] Benzi F, Davoli I, Rovezzi M and d'Acapito F 2008 *Rev. Sci. Instrum.* **79** 103902 URL <http://www.esrf.eu/computing/scientific/CARD/CARD.html>
- [13] Costanzo T, Benzi F, Ghigna P, Pin S, Spinolo G and d'Acapito F 2014 *J. Synchrotron Rad.* **21** 395
- [14] Ravel B and Newville M 2005 *J. Synchrotron Rad.* **12** 537
- [15] McKale A G, Veal B W, Paulikas A P, Chan S K and Knapp G S 1988 *Phys. Rev. B* **38**
- [16] d'Acapito F, Souchier E, Noe P, Blaise P, Bernard M and Jousseume V 2015 *Phys. Status Solidi A* Submitted
- [17] Celano U *et al.* 2014 *Nano Lett.* **14** 2401